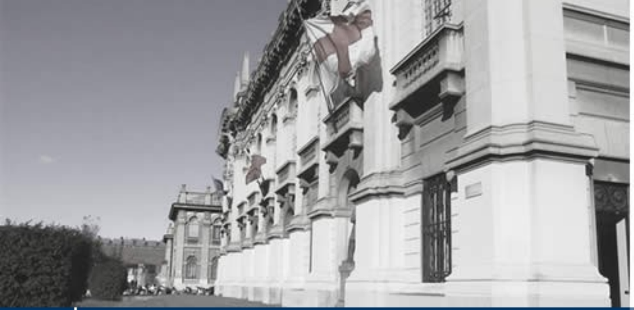

POLITECNICO DI MILANO





Investigation of on-line tumor edge detection using multiple Bragg peak detection in carbon therapy.

Marta F. Dias

Charles-Antoine Collins Fekete, Guido Baroni, Marco Riboldi, Joao Seco

Challenges in charged particle therapy

→ Charged particles, e.g. carbons are highly sensitive to tissue density variations.

e.g.:

400MeV/u carbon beam crosses 27.3cm of water but only 16.4cm of bone

So 1mm of bone in a water medium causes an error of 0.6mm

Challenges in charged particle therapy

→ Charged particles, e.g. carbons are highly sensitive to tissue density variations.

e.g.:

400MeV/u carbon beam crosses 27.3cm of water but only 16.4cm of bone

So 1mm of bone in a water medium causes an error of 0.6mm

→ Tumor shifts/shrinkage geographical miss and/or high-dose deposition at OARs.

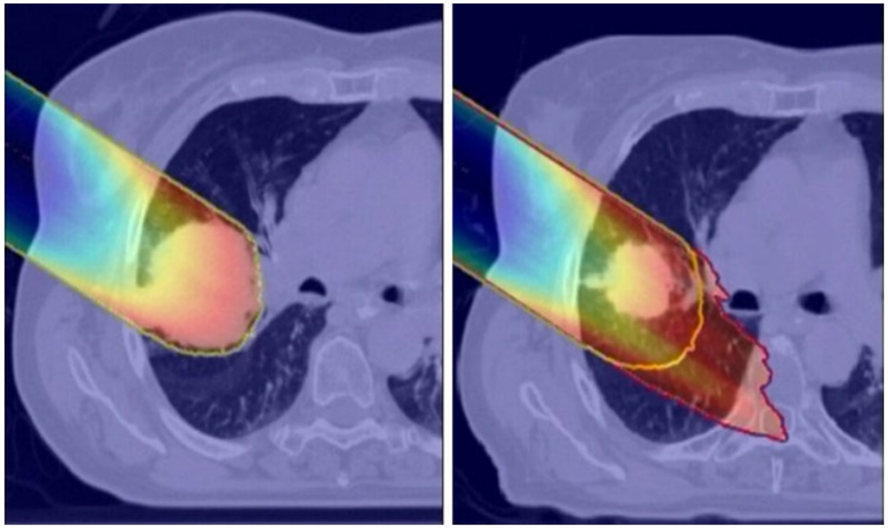

Image from Mori *et al.* [2013]

Challenges in charged particle therapy

It is crucial to have on-line/precise knowledge of edges/interfaces along carbon's path!

→ Tumor shifts/shrinkage geographical miss and/or high-dose deposition at OARs.

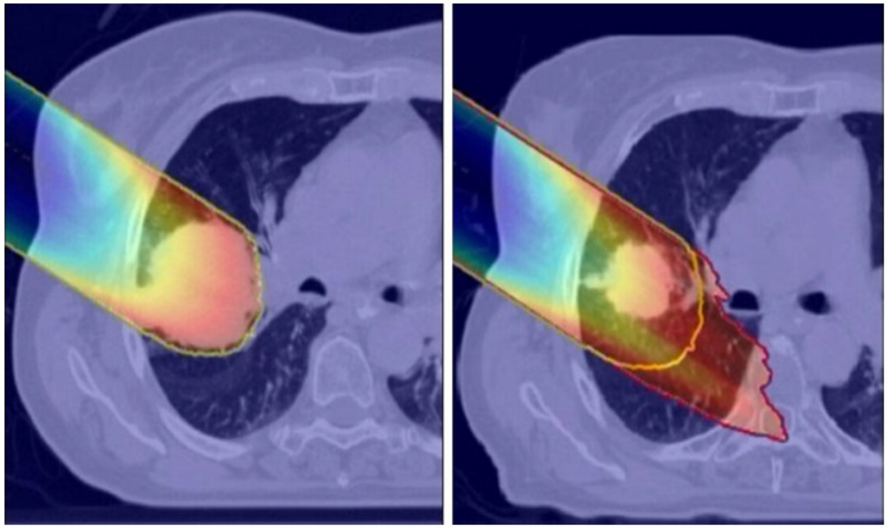

Image from Mori *et al.* [2013]

Possible Solution: Carbon Imaging

→ Carbon CT/Radiography

Possible Solution: Carbon Imaging

→ Carbon CT/Radiography

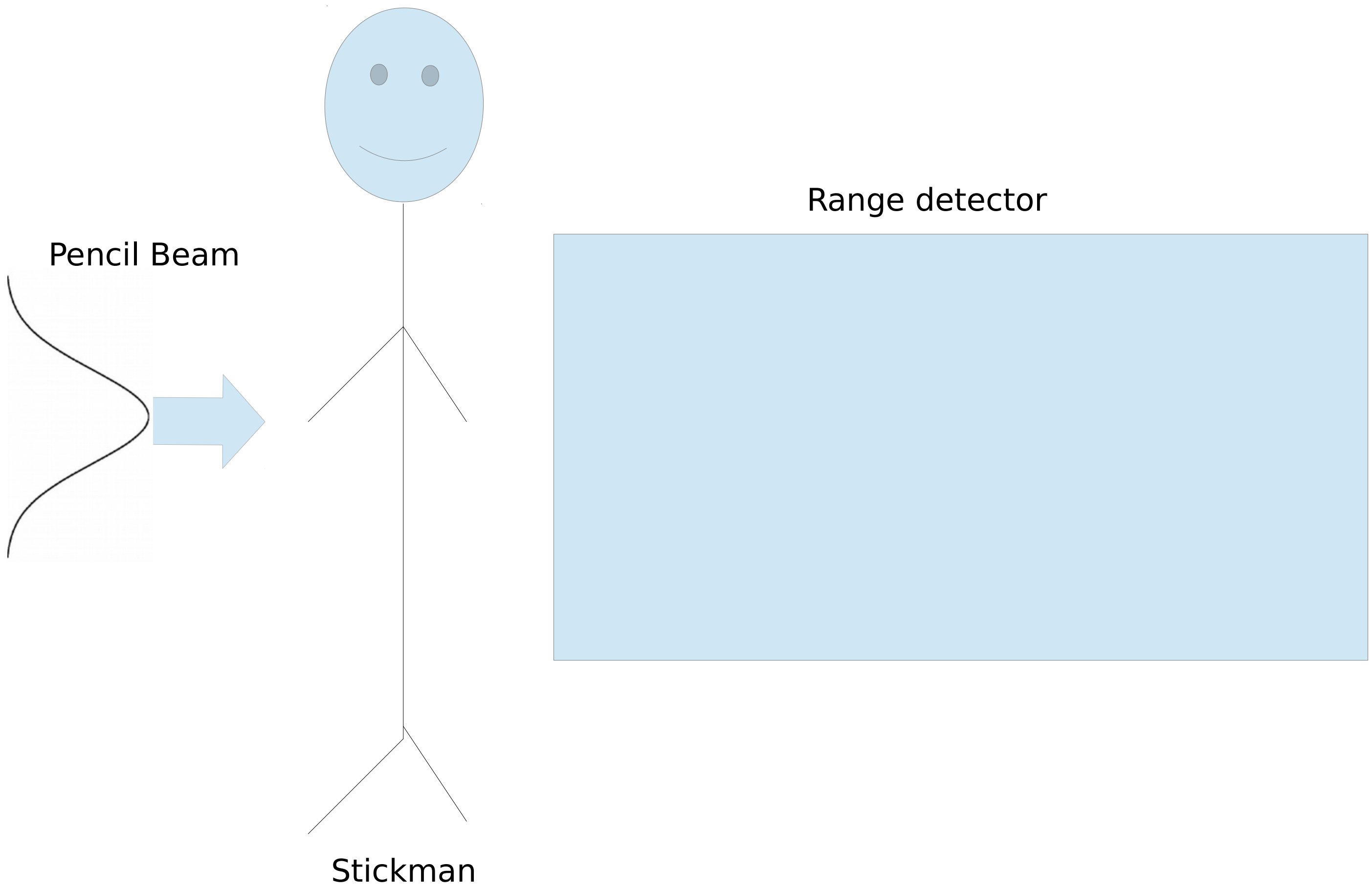

Possible Solution: Carbon Imaging

→ Carbon CT/Radiography

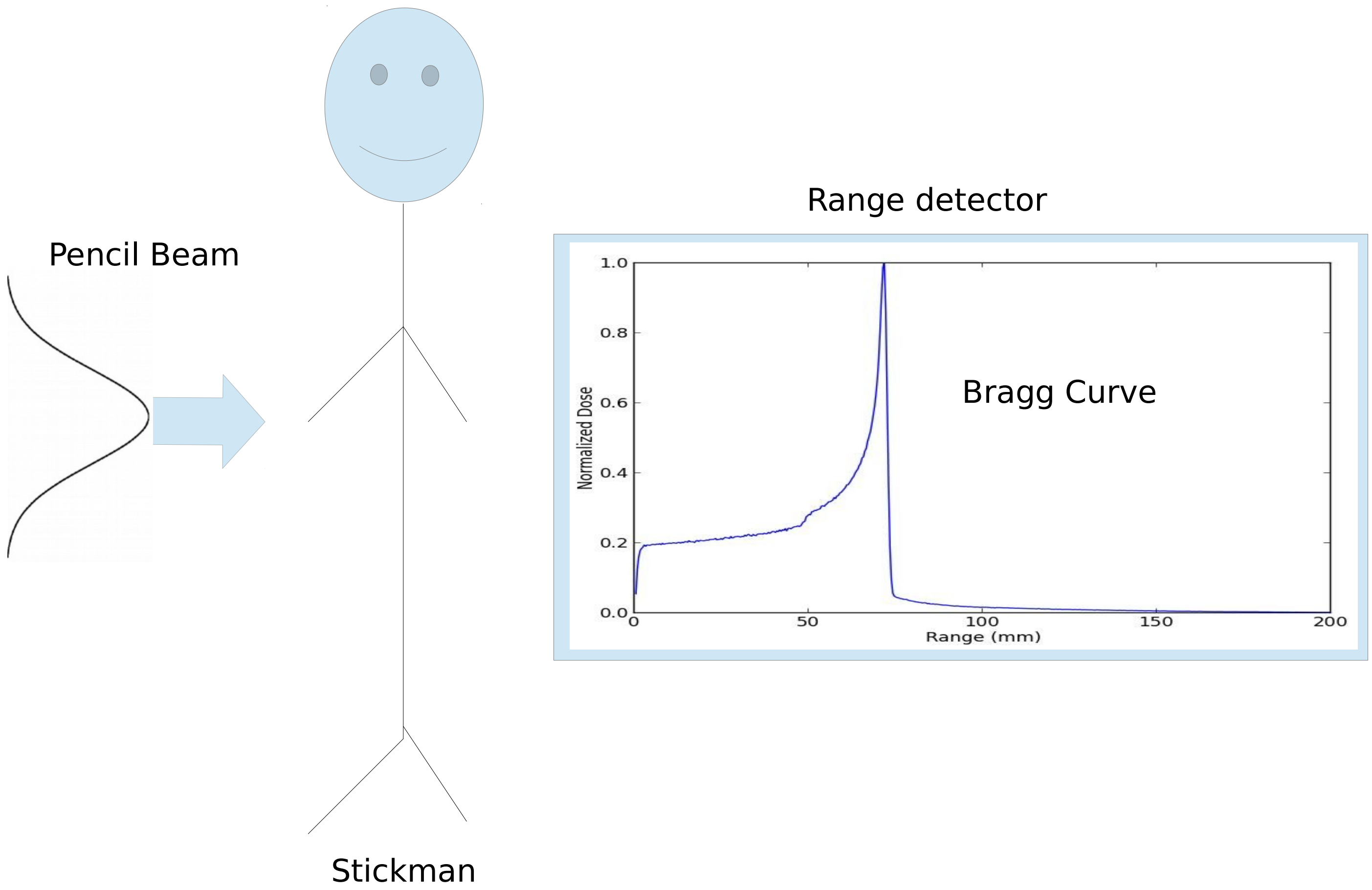

Possible Solution: Carbon Imaging

→ Carbon CT/Radiography

Bragg Peak position is converted into total WET crossed.

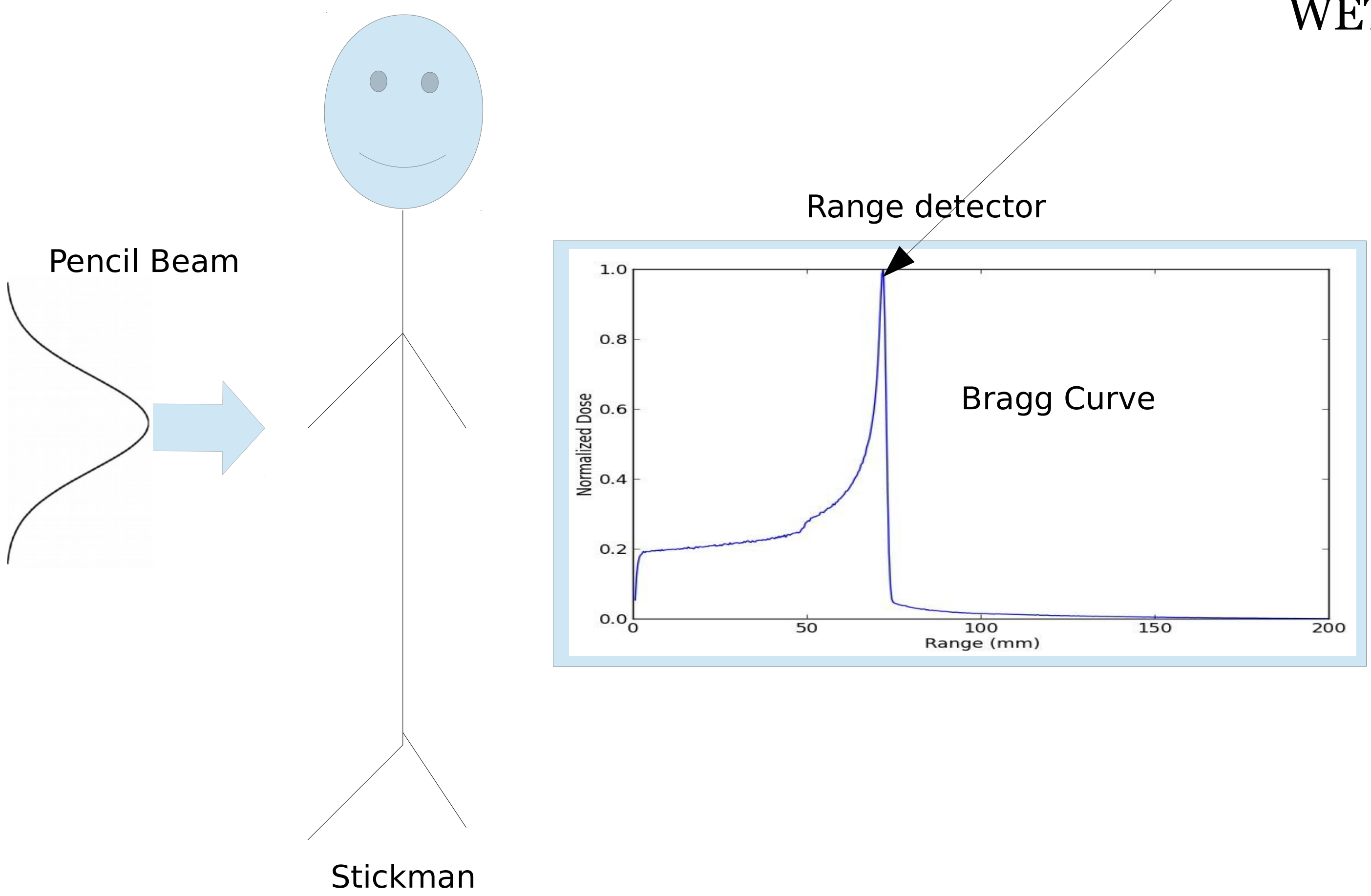

Possible Solution: Carbon Imaging

→ Carbon CT/Radiography

Bragg Peak position is converted into total WET crossed.

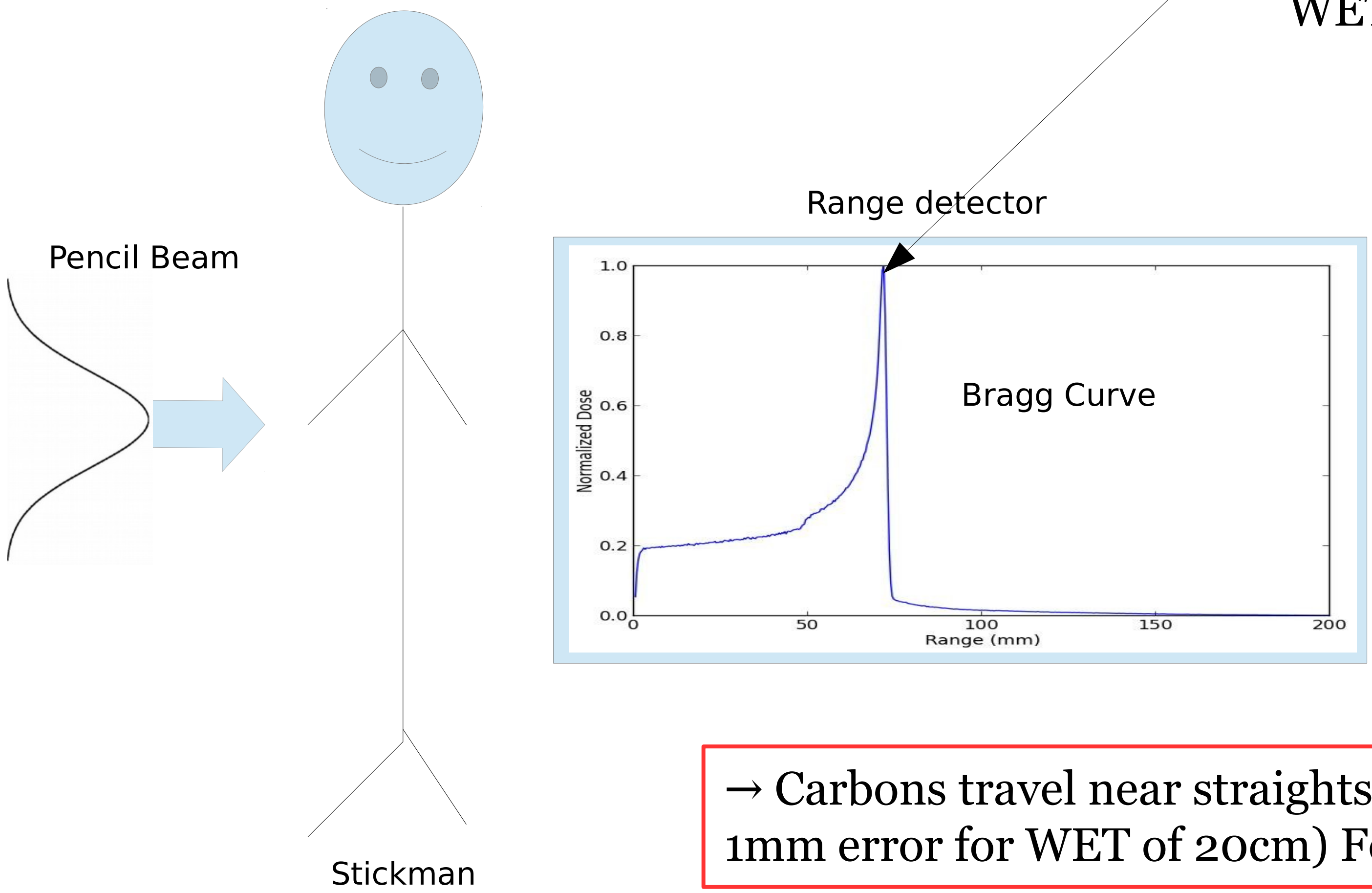

→ Carbons travel near straights paths (less than 1mm error for WET of 20cm) Fekete *et al.* [2016]

Each peak contains information about the crossed materials

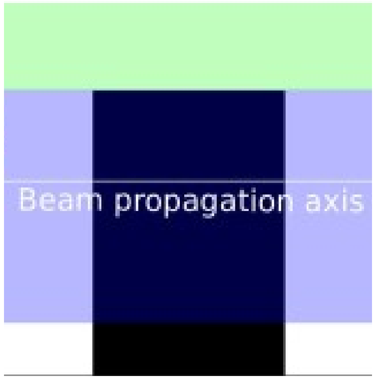

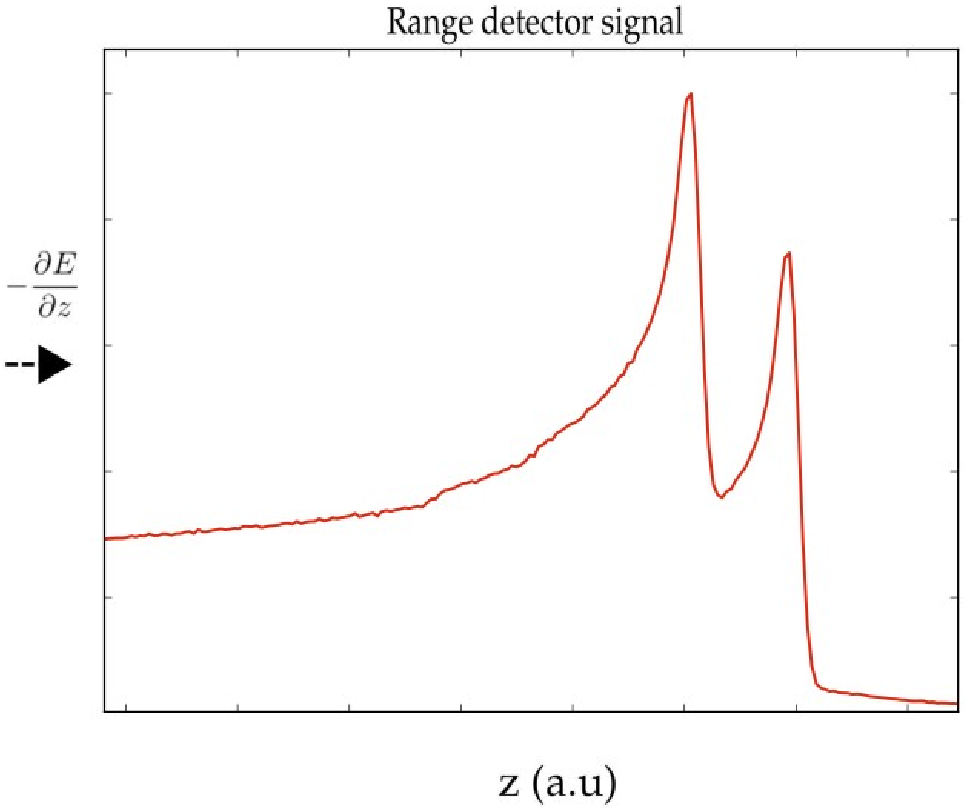

It is crucial to have on-line/precise knowledge of edges/interfaces along carbon's path!

Hypothesis: we can detect on-line (during treatment) tumor edges using information from the detected multiple Bragg peaks.

- Reduced number of irradiation beams in order to reduce dose delivered to the patient.
- No imaging reconstruction methods.

➔We can decompose the peak into pristine Bragg peaks.

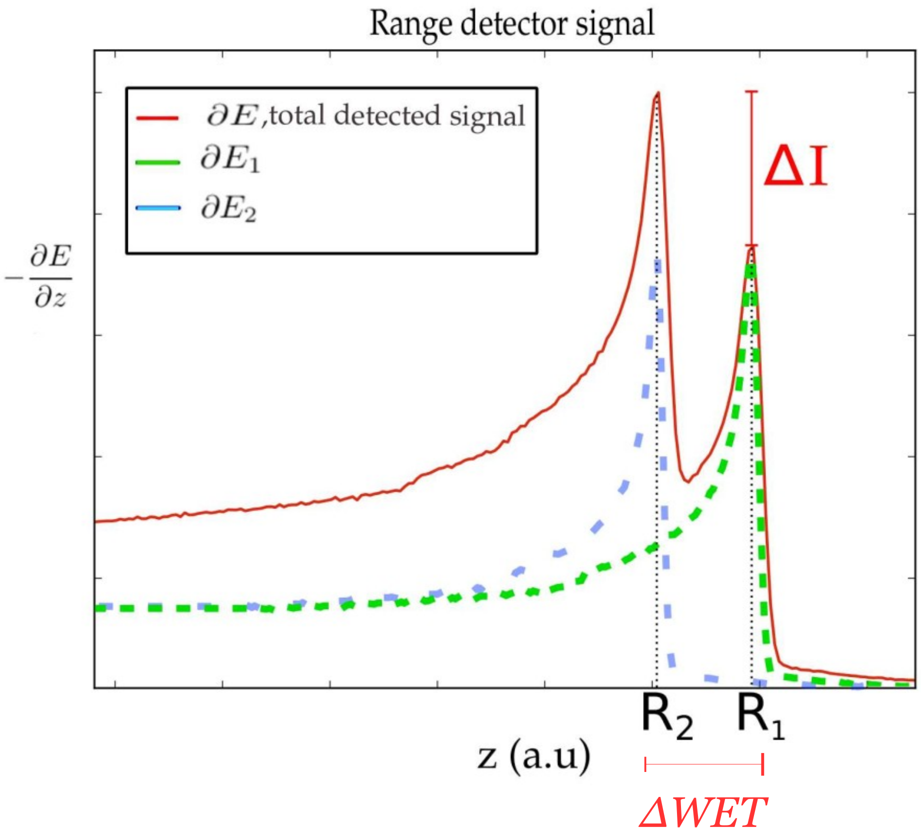

➔We can decompose the peak into pristine Bragg peaks.

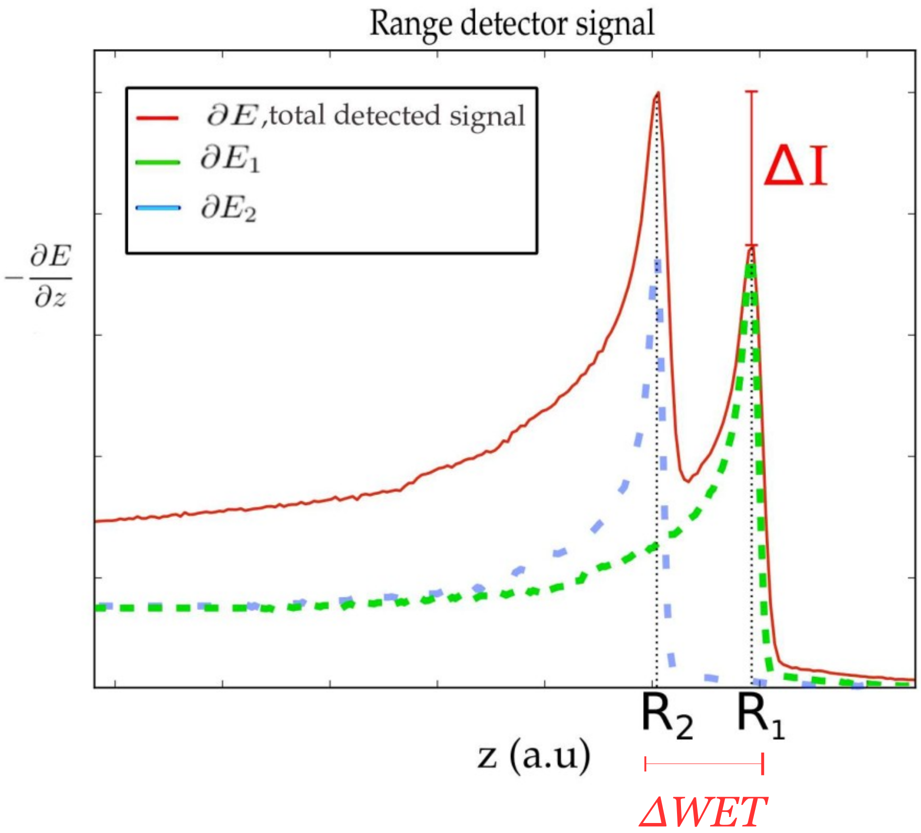

Assumptions:

1. Straight path;

→We can decompose the peak into pristine Bragg peaks.

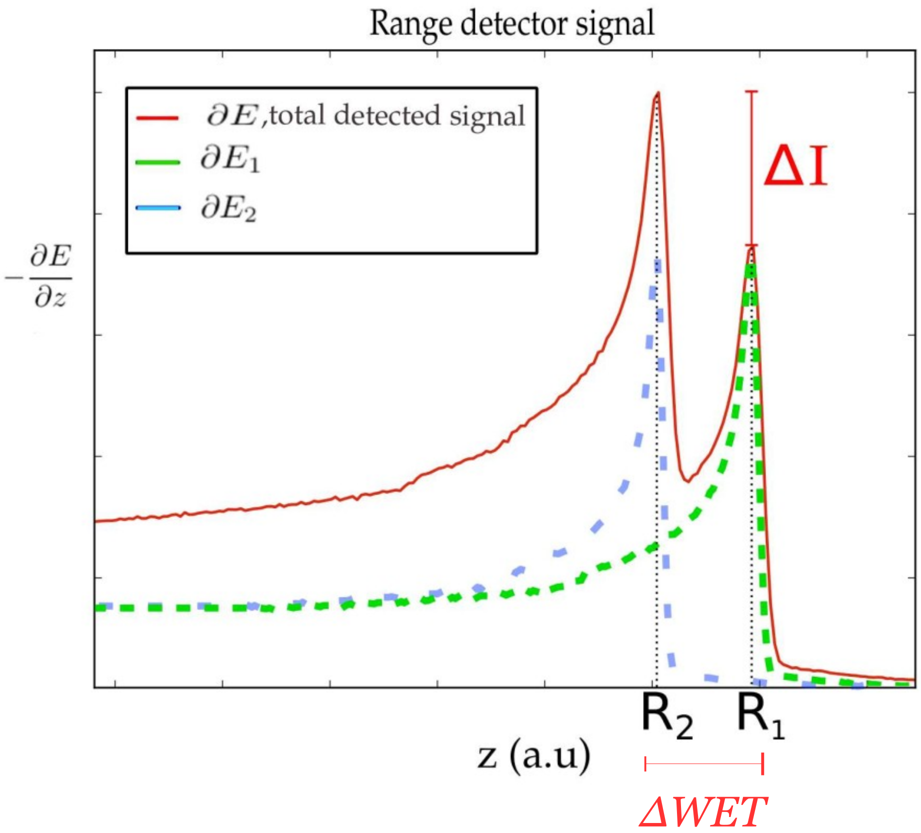

Assumptions:

1. Straight path;

2. No tails due to secondary particles.

➔We can decompose the peak into pristine Bragg peaks.

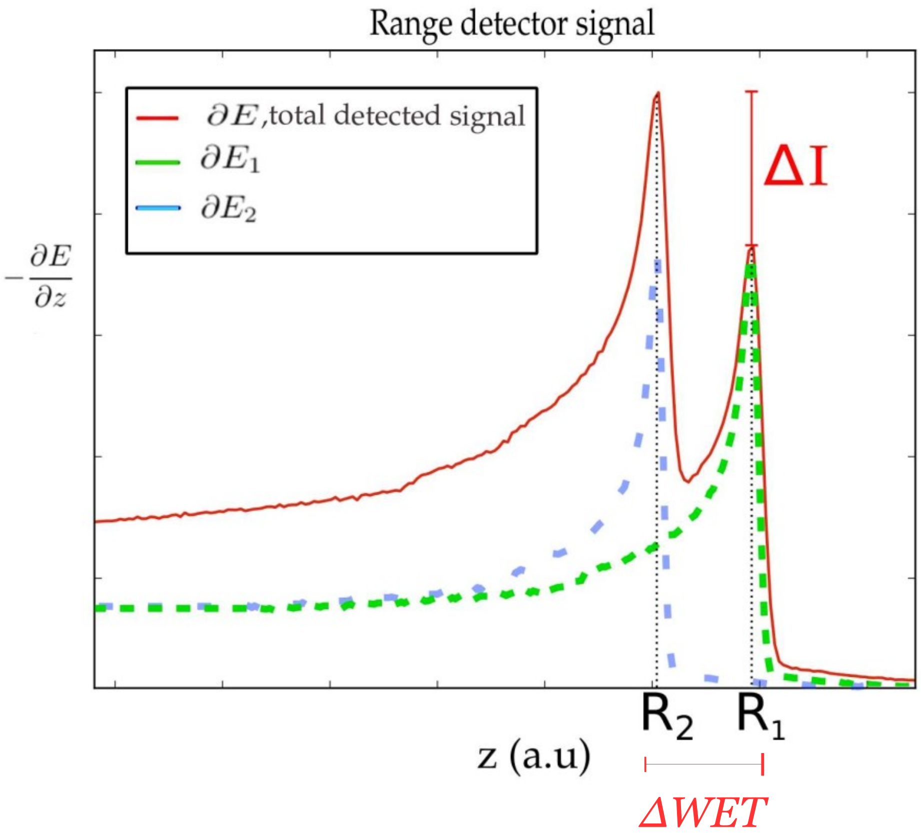

Assumptions:

1. Straight path;
2. No tails due to secondary particles.
3. Gaussian Beam, this is assumed to be valid at any depth along the beam trajectory.

➔We can decompose the peak into pristine Bragg peaks.

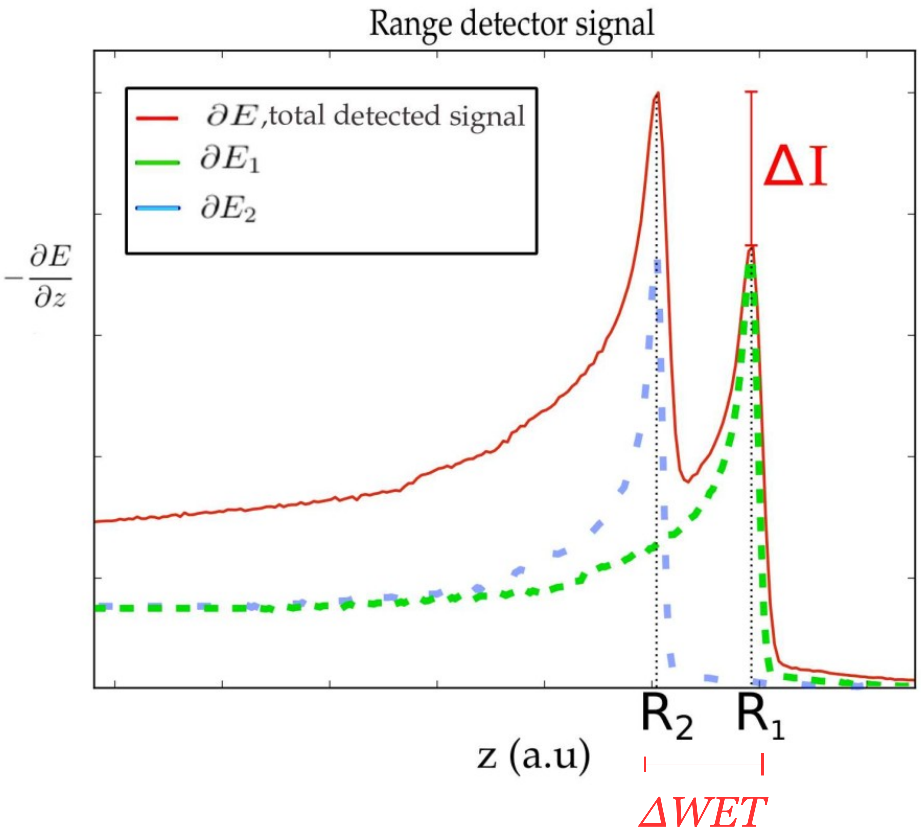

Assumptions:

1. Straight path;

2. No tails due to secondary particles.

3. Gaussian Beam, this is assumed to be valid at any depth along the beam trajectory.

4. $R_1 = \alpha E_0^{\,p}$ (Bortfeld and Schlegel, [1996])

→We can decompose the peak into pristine Bragg peaks.

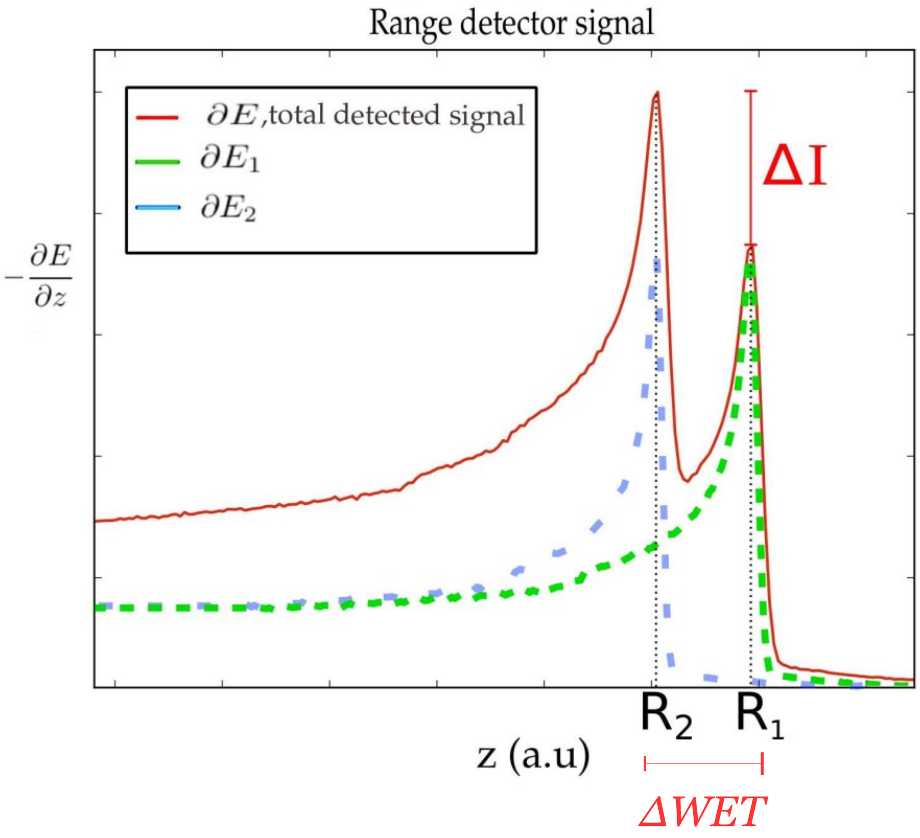

Assumptions:

1. Straight path;
2. No tails due to secondary particles.
3. Gaussian Beam, this is assumed to be valid at any depth along the beam trajectory.
4. $R_1 = \alpha E_o^{\,p}$ (Bortfeld and Schlegel, [1996])

The dose deposit at any point z<R:

$$-\frac{\partial E}{\partial z} = \frac{(R-z)^{1/p-1}}{p\alpha^{1/p}}$$

→We can decompose the peak into pristine Bragg peaks.

$$\Delta I = \frac{\partial E(R_2) - \partial E(R_1)}{\partial E(R_1)}$$

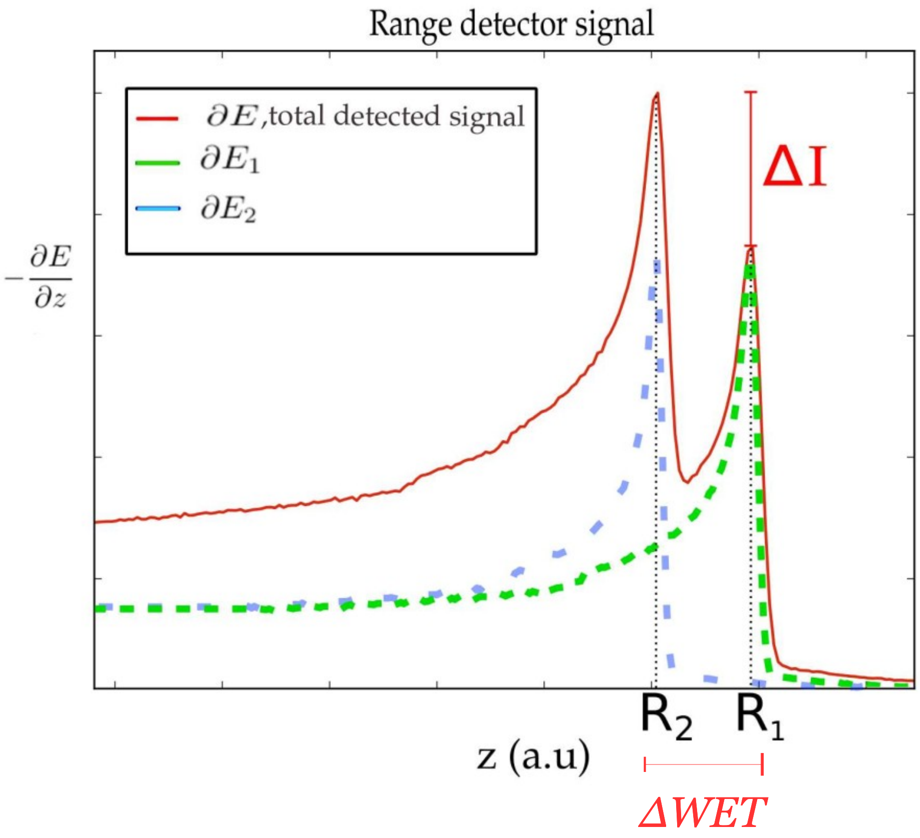

➔We can decompose the peak into pristine Bragg peaks.

$$\Delta I = \frac{\partial E(R_2) - \partial E(R_1)}{\partial E(R_1)}$$

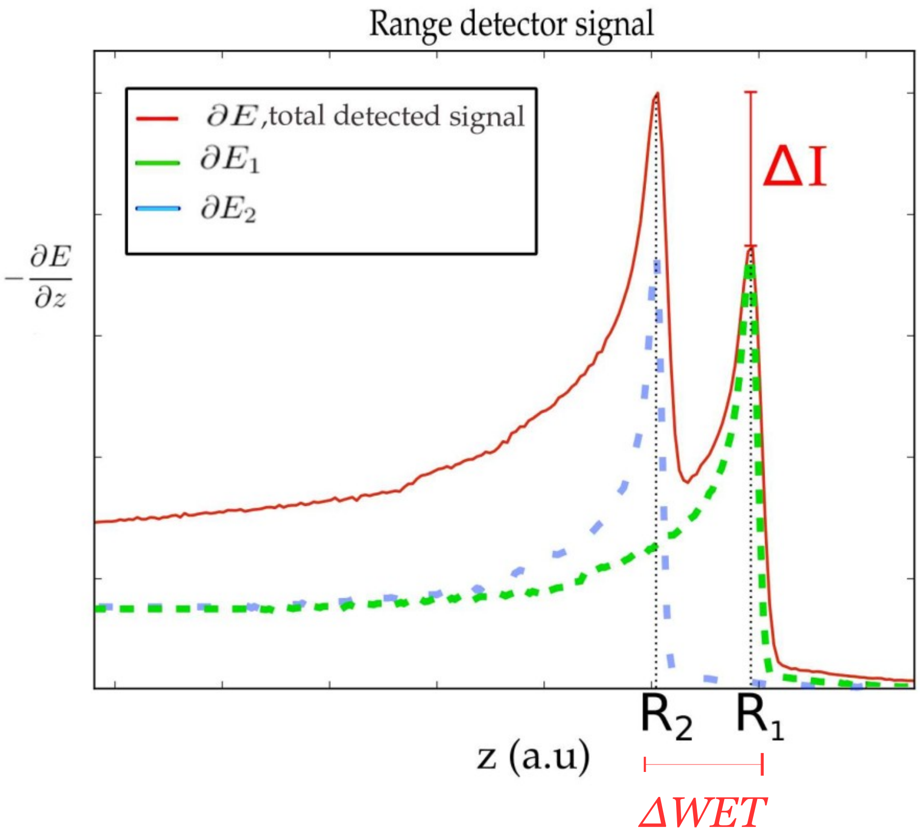

Theoretical *ΔI–ΔWET* curve

$$\Delta I = \lambda^{1-\frac{1}{p}} \Delta WET^{\frac{1}{p}-1} + \left(\frac{W_2}{W_1} - 1\right)$$

- We can decompose the peak into pristine Bragg peaks.

$$\Delta I = \frac{\partial E(R_2) - \partial E(R_1)}{\partial E(R_1)}$$

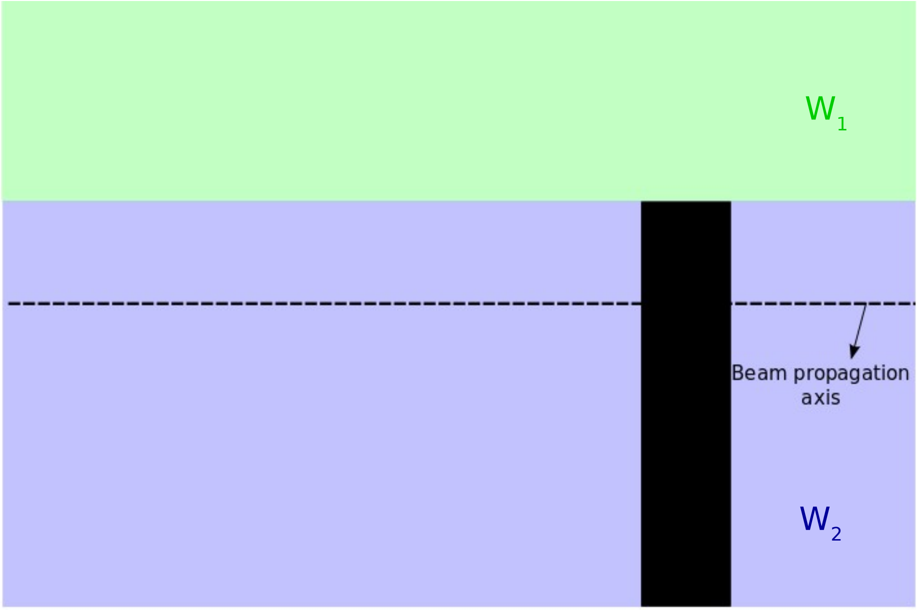

Theoretical *ΔI–ΔWET* curve

$$\Delta I = \lambda^{1-\frac{1}{p}} \Delta WET^{\frac{1}{p}-1} + \left(\frac{W_2}{W_1} - 1\right)$$

W_1 → percentage of carbons crossing above the interface

➔We can decompose the peak into pristine Bragg peaks.

$$\Delta I = \frac{\partial E(R_2) - \partial E(R_1)}{\partial E(R_1)}$$

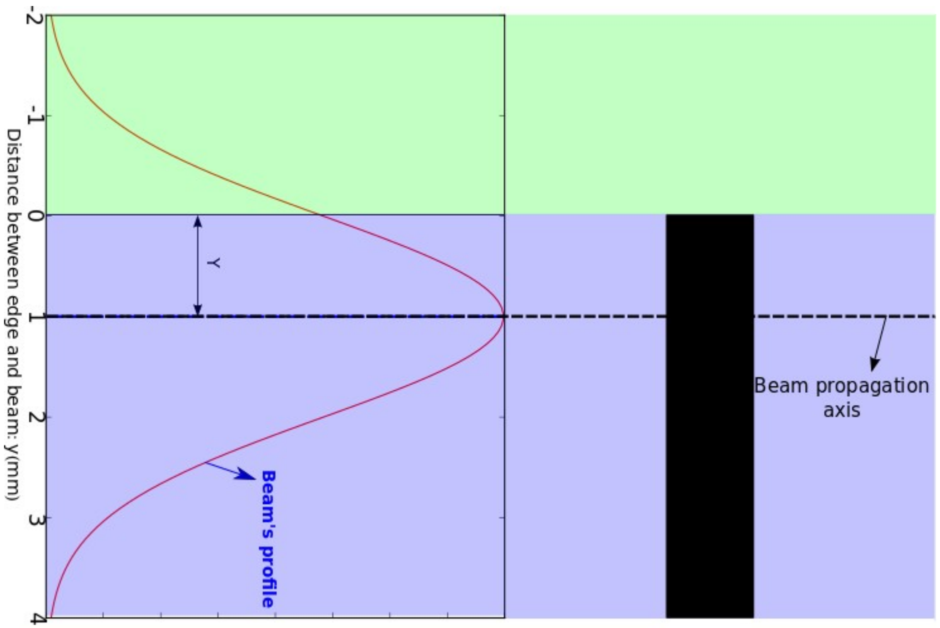

Theoretical *ΔI–ΔWET* curve

$$\Delta I = \lambda^{1-\frac{1}{p}} \Delta WET^{\frac{1}{p}-1} + \left(\frac{W_2}{W_1} - 1\right)$$

W_1 → percentage of carbons crossing above the interface

$$W_2 = 1 - W_1 \rightarrow W_1 = \frac{1 - erf\left(\frac{Y}{\sigma\sqrt{2}}\right)}{2}$$

2. Materials and Methods

➔We can decompose the peak into pristine Bragg peaks.

$$\Delta I = \frac{\partial E(R_2) - \partial E(R_1)}{\partial E(R_1)}$$

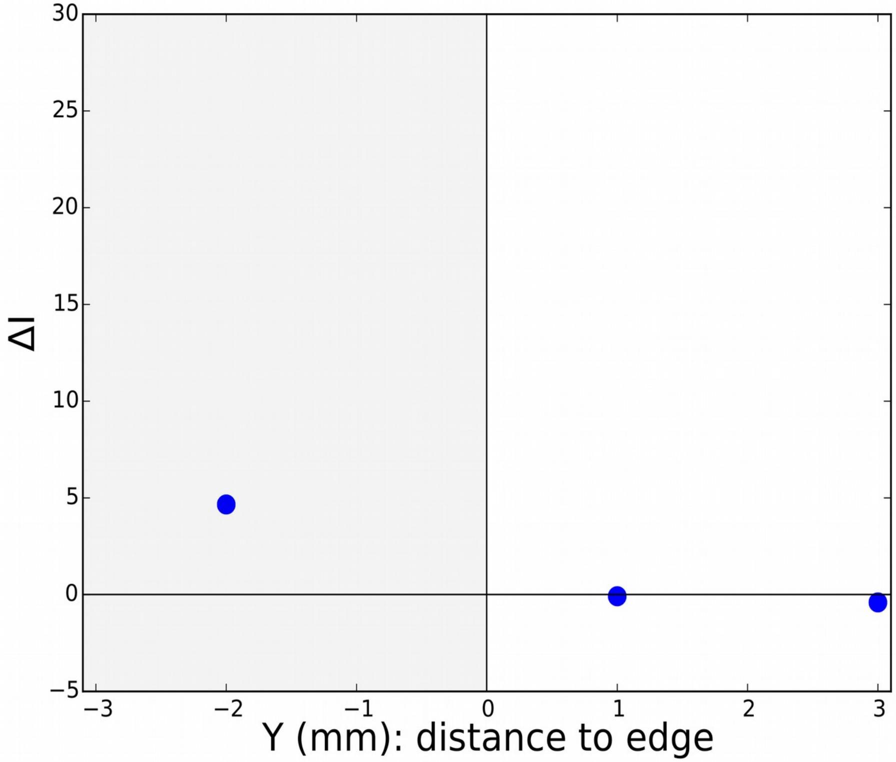

Theoretical *ΔI–ΔWET* curve

$$\Delta I = \lambda^{1-\frac{1}{p}} \Delta WET^{\frac{1}{p}-1} + \left(\frac{W_2}{W_1} - 1\right)$$

W_1 → percentage of carbons crossing above the interface

$$W_2 = 1 - W_1 \rightarrow W_1 = \frac{1 - erf\left(\frac{Y}{\sigma\sqrt{2}}\right)}{2}$$

➔ We scan the interface for three irradiation spots (known spacing).

→We can decompose the peak into pristine Bragg peaks.

$$\Delta I = \frac{\partial E(R_2) - \partial E(R_1)}{\partial E(R_1)}$$

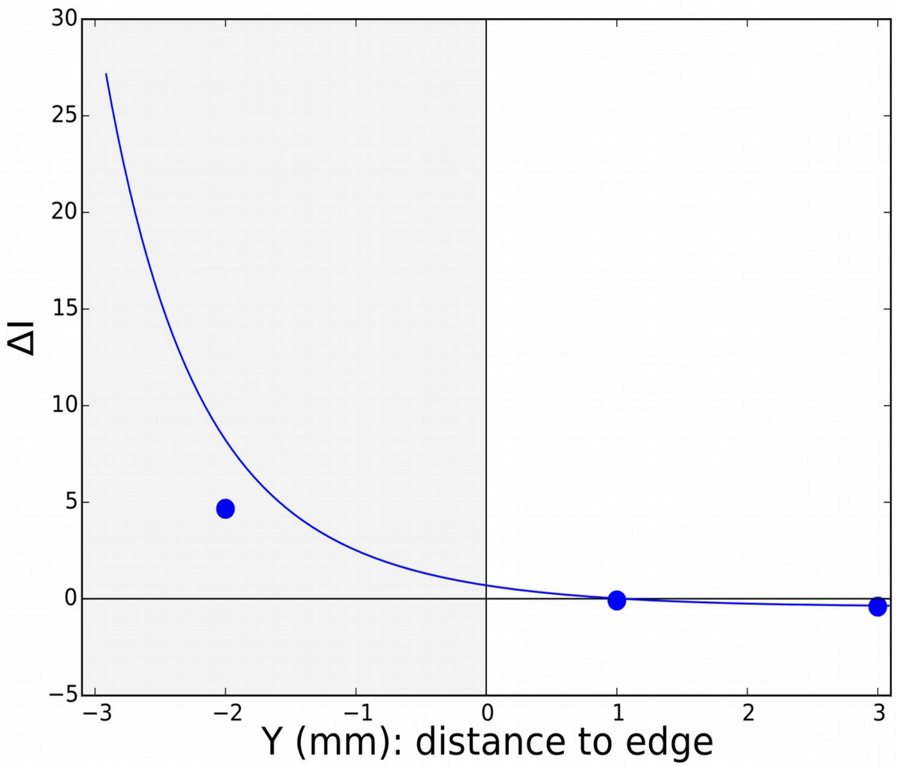

Theoretical *ΔI–ΔWET* curve

$$\boxed{\Delta I = \lambda^{1-\frac{1}{p}} \Delta WET^{\frac{1}{p}-1} + \left(\frac{W_2}{W_1} - 1\right)}$$

W_1 → percentage of carbons crossing above the interface

$$W_2 = 1 - W_1 \rightarrow W_1 = \frac{1 - erf\left(\frac{Y}{\sigma\sqrt{2}}\right)}{2}$$

→ We scan the interface for three irradiation spots (known spacing).

→Apply the fit

2. Materials and Methods

➔We can decompose the peak into pristine Bragg peaks.

$$\Delta I = \frac{\partial E(R_2) - \partial E(R_1)}{\partial E(R_1)}$$

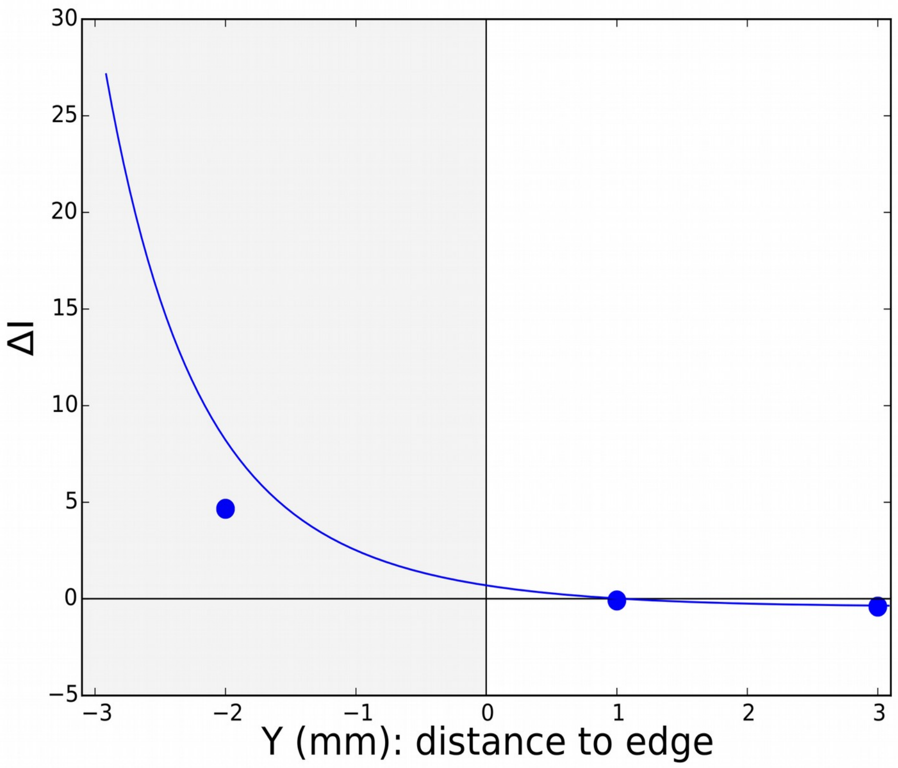

Theoretical *ΔI–ΔWET* curve

$$\Delta I = \lambda^{1-\frac{1}{p}} \Delta WET^{\frac{1}{p}-1} + \left(\frac{W_2}{W_1} - 1\right)$$

0

➔ At the edge:

$$\Delta I = \lambda^{1-\frac{1}{p}} \Delta WET^{\frac{1}{p}-1}$$

Validation: Monte Carlo Simulations

- 400 MeV carbon beam with $n=10^6$ particles
- Geant4 (v 4.9.6.p02) (Agostinelli *et al.* [2003]). Ion packages (Lechner *et al.* [2010]).
- FWHM = 4mm, 8mm and 10mm

Parametric phantoms:

Rectangular bone insert

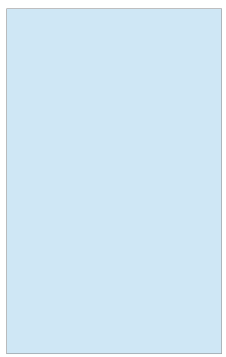

Semi-cylindrical bone insert

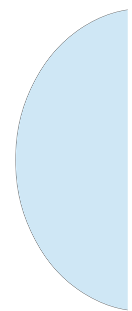

- Beam position: [-3,-2,-1,0,1,2,3]mm above and below the interface

Parametric phantoms:

Rectangular bone insert

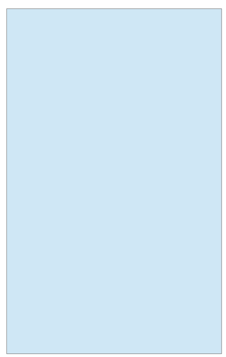

Semi-cylindrical bone insert

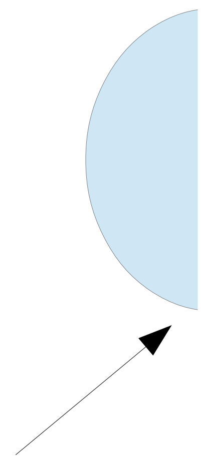

Range dilution effects, due to carbons from the same beam crossing different

- Beam position: [-3,-2,-1,0,1,2,3]mm above and below the interface

Edge detection through multiple BP: lung tumor example

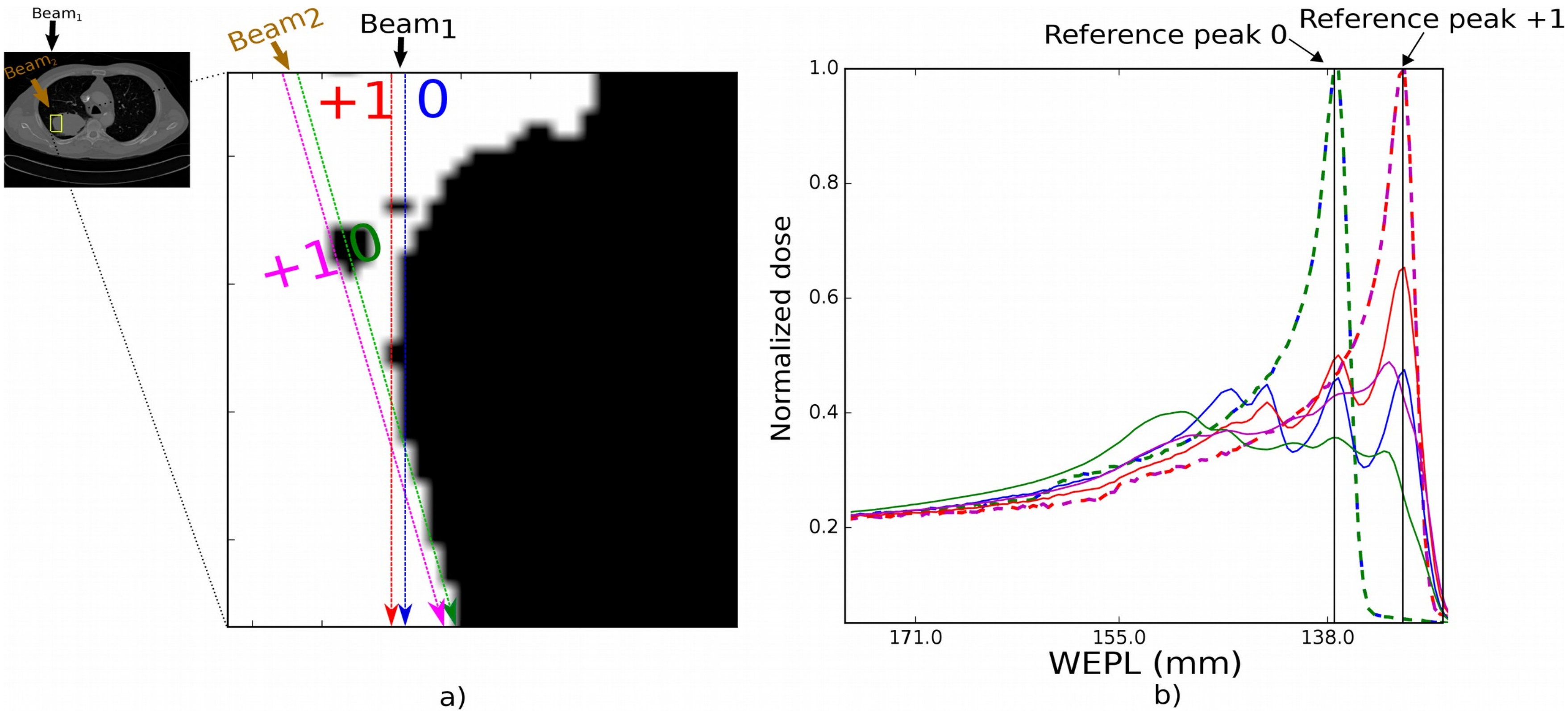

→ X-ray CT prior knowledge for peak identification

→ The WET crossed and expected BP can be computed.

Parametric phantoms:

Parallel interface

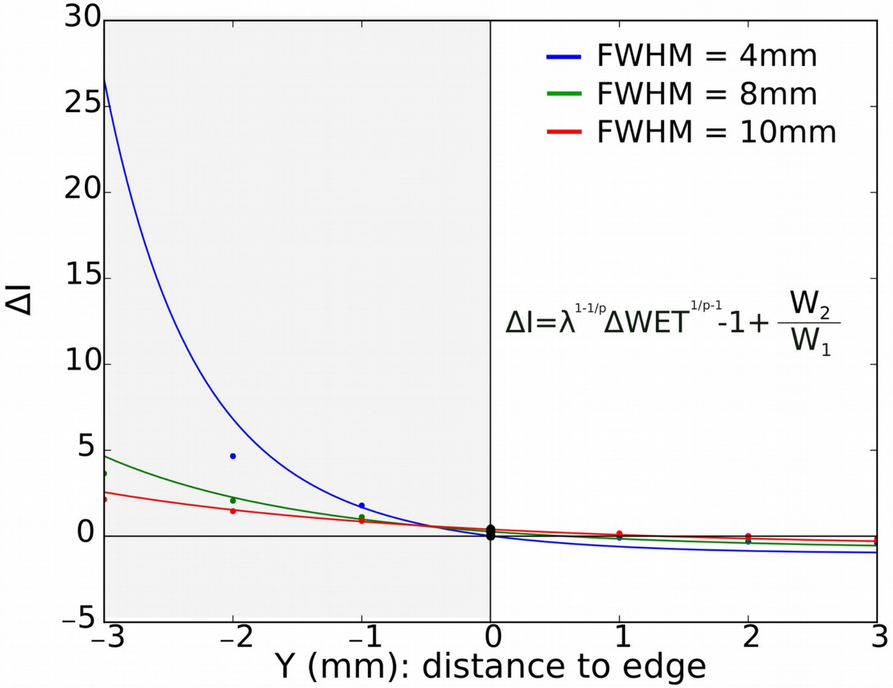

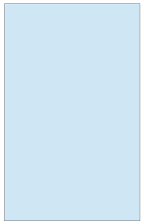

Semi-cylindrical

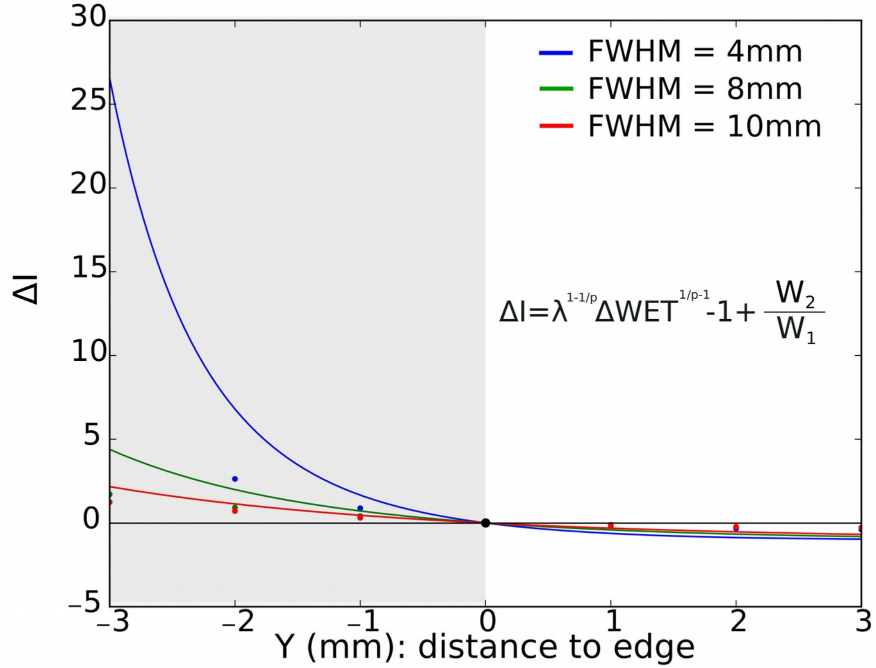

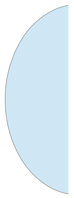

Parametric phantoms:

Parallel interface

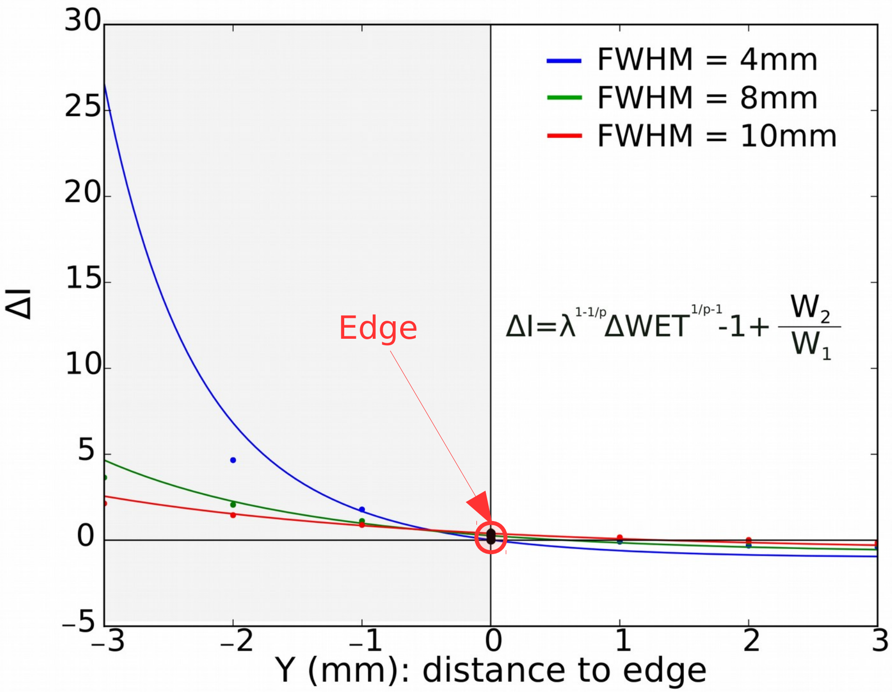

Semi-cylindrical

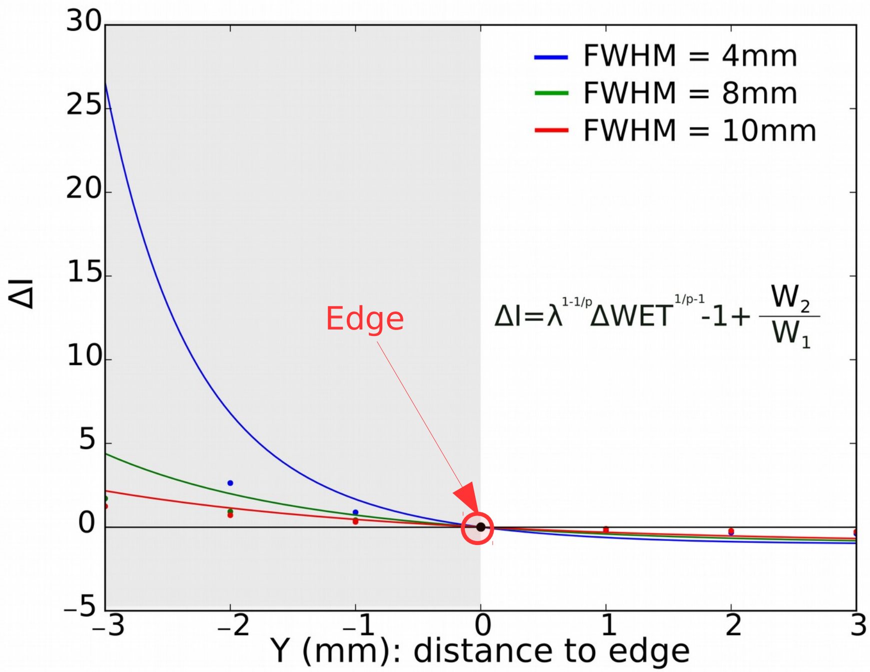

$$\Delta I = \lambda^{1-\frac{1}{p}} \Delta WET^{\frac{1}{p}-1}$$ → Zero at: 0.001mm

Parametric phantoms:

Parallel interface

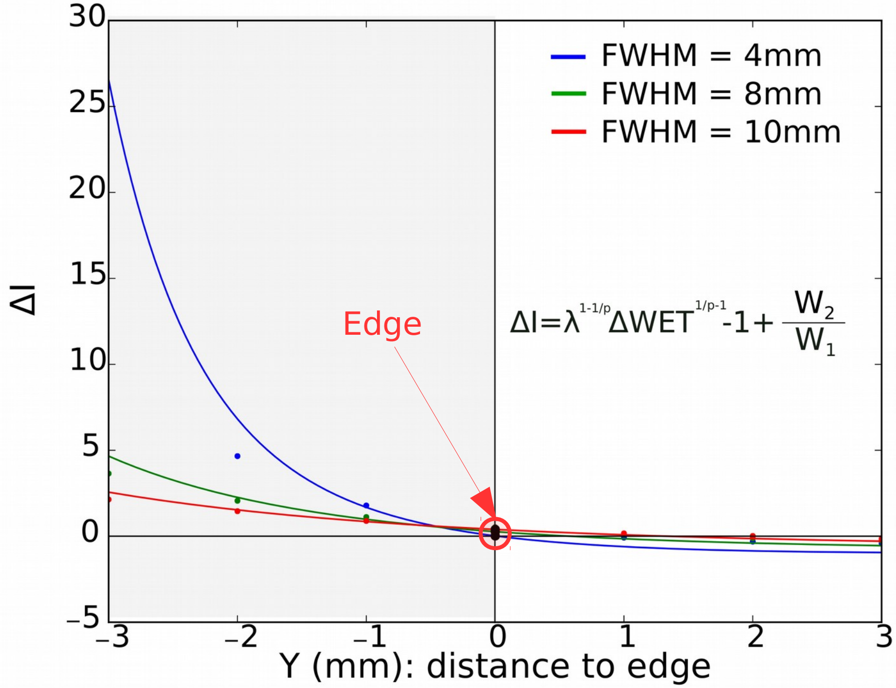

Semi-cylindrical

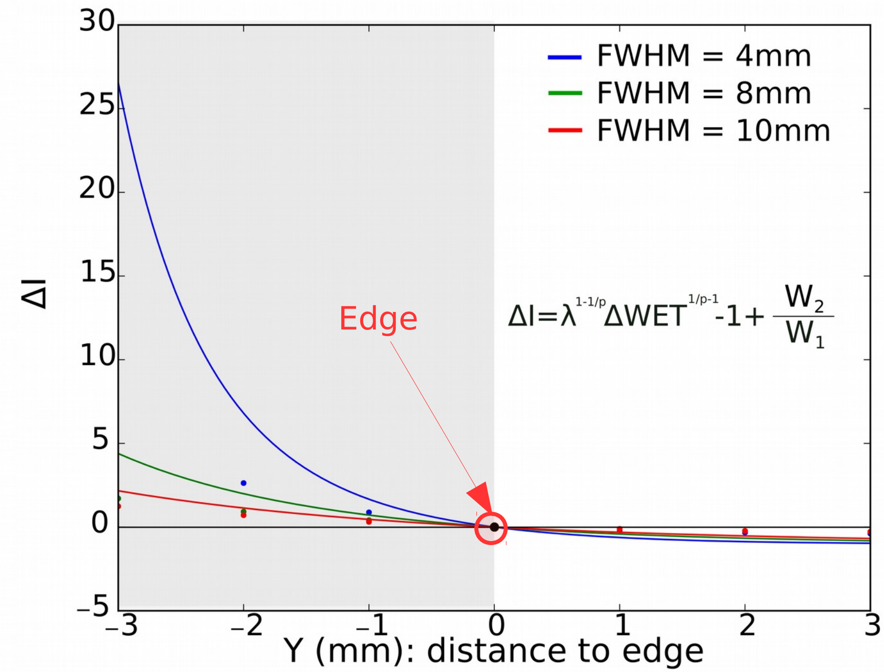

→ Same error for all FWHM
→ Larger FWHM easier to identify the peaks

Clinical environment: Lung tumor

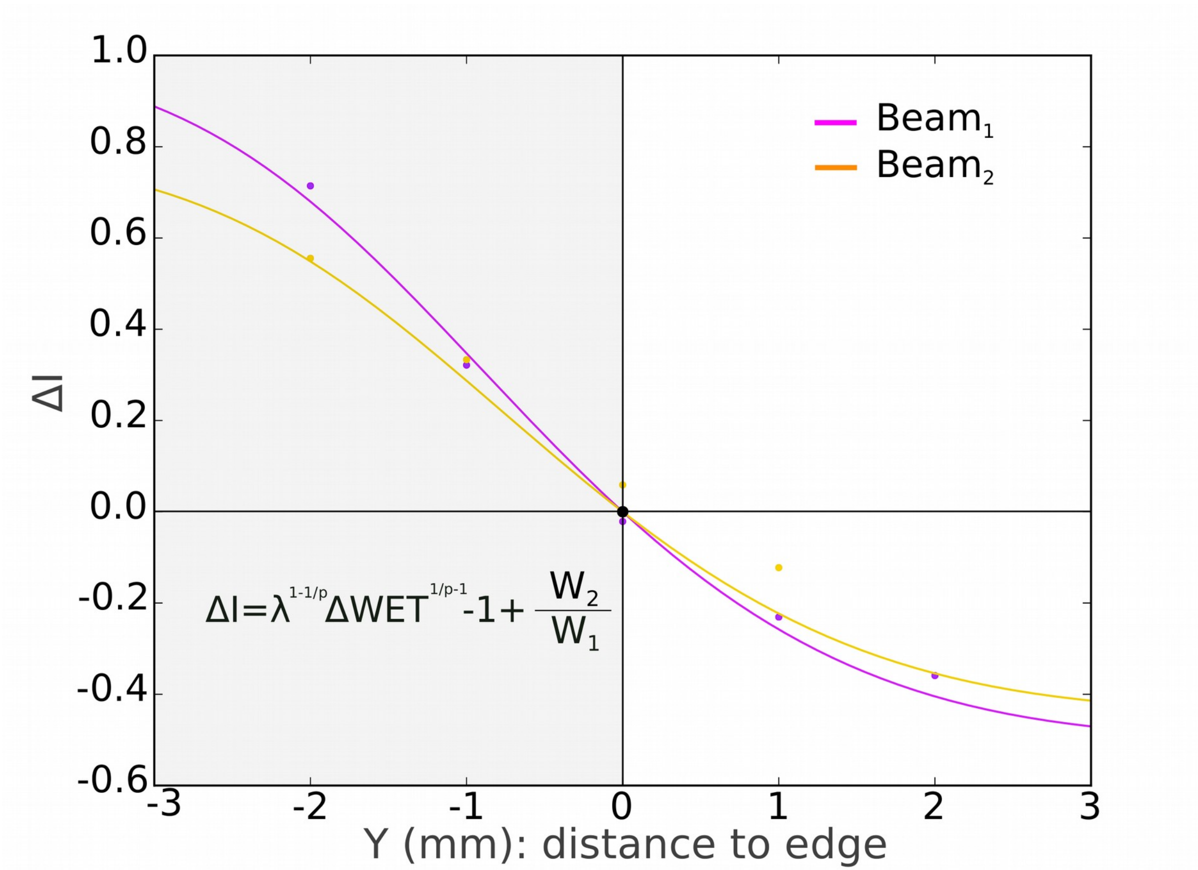

Clinical environment: Lung tumor

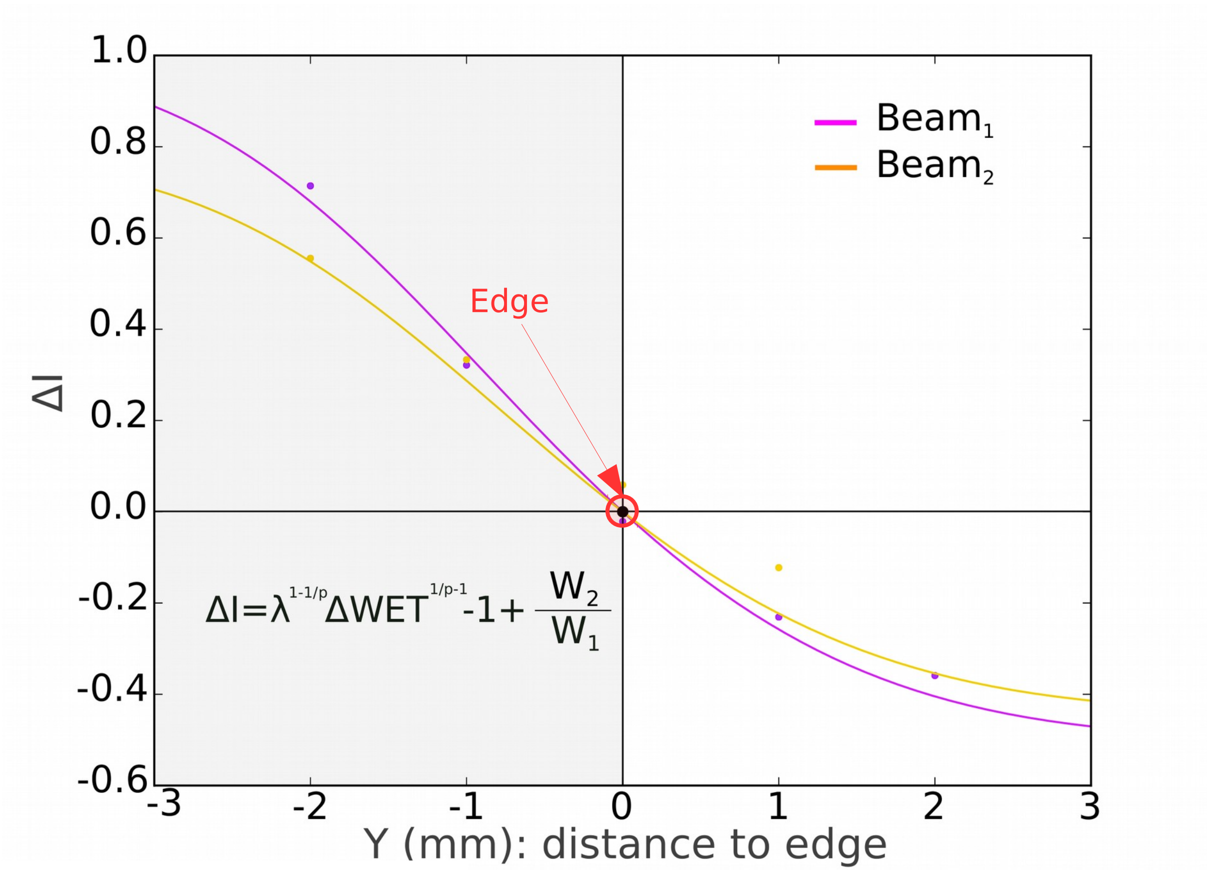

$$\Delta I = \lambda^{1-\frac{1}{p}} \Delta WET^{\frac{1}{p}-1}$$ → Zero at: 0.001/-0.015mm

5. Conclusions and Future work

Edge detection within <0.01mm accuracy using multiple BP information.

→ Carbon imaging is worse than helium imaging [Fekete *et al.* 2016];

5. Conclusions and Future work

Edge detection within <0.01mm accuracy using multiple BP information.

→ Carbon imaging is worse than helium imaging [Fekete *et al.* 2016];

→ Difficult to change particle type and if two beams available, it is possible on-line detection;

Edge detection within <0.01mm accuracy using multiple BP information.

→ Carbon imaging is worse than helium imaging [Fekete *et al.* 2016];

→ Difficult to change particle type and if two beams available, it is possible on-line detection;

→ Low dose to the patient;

6. Conclusions and Future work

Edge detection within <0.01mm accuracy using multiple BP information.

→ Carbon imaging is worse than helium imaging [Fekete *et al.* 2016];

→ Difficult to change particle type and if two beams available, it is possible on-line detection;

→ Low dose to the patient;

→ Prior-knowledge strategies are required for the identification of the relevant peaks;

→ Future work will consider applying the same methods to other tumor areas and structures which can be used for patient positioning.

Acknowledgements

Fundação para a Ciência e a Tecnologia
Grant SFRH / BD / 85749 / 2012

German Cancer Research Center

Politecnico di Milano

Computer Aided RadioTherapy & Computer Aided Surgery

Massachusetts General Hospital

References

Fekete CA, Volz L., Portillo S and Seco, J.A theoretical framework to predict the most likely ion path in particle imaging, arXiv:1610.05774, 2016
A. Lechner, V.N. Ivanchenko, J. Knobloch. *Validation of recent Geant4 physics models for application in carbon ion therapy* Nuclear Instruments and Methods in Physics Research B (268). Pages 2343–2354., April 2010.

H Muraishi, K Nishimura, S Abe, *et al*. *Heavy Ion CT System Based on the Measurement of Residual Range Distribution: Improvement of the Optical Detector System*. Pages 4354–4358, 2007.

I Rinaldi, S Brons, J Gordon, R Panse, and B Voss. *Experimental characterization of a prototype detector system for carbon ion radiography and tomography*. 413, 2013

I Rinaldi, S Brons, O Jakel, B Voss, and K Parodi. *Experimental investigations on carbon ion scanning radiography using a range telescope*. Physics in medicine and biology, 59(12):3041–57, June 2014.

K Clark, B Vendt, K Smith, J Freymann, J Kirby, P Koppel, S Moore, S Phillips, D Maffitt, M Pringle, L Tarbox, F Prior. *The Cancer Imaging Archive (TCIA): Maintaining and Operating a Public Information Repository*, Journal of Digital Imaging, Volume 26, Number 6, December, 2013, pp 1045-1057.

R. F. Hurley, R.W. Schulte, V. A. Bashkirov, H. F.-W. Sadrozinski, V. Rykalin and G. Coutrakon, P. Koss and B. Patyal, *Water-equivalent path length calibration of a prototype proton CT scanner*. Med. Phys. 39 (5), May 2012

S. Agostinelli, J. Allison, K. Amako, *et al*. *Geant4—a simulation toolkit*. Nuclear Instruments and Methods in Physics Research Section A: Accelerators, Spectrometers, Detectors and Associated Equipment, 506(3):250–303, July 2003.

Schneider U, Pedroni E and Lomax A 1996 The calibration of CT Hounsfield units for radiotherapy treatment planning Phys. Med. Biol. 41 111–124

Shinichiro Mori, Silvan Zenklusen and Antje-Christin Knopf, Current status and f*uture prospects of multi-dimensional image-guided particle therapy*. *Radiol Phys Technol, 6:249–272, 20*13thoracic cancers. Journal of Radiation Research,

Shinichiro Mori, Lei Dong, George Starkschall, R*adhe Mohan and George T.Y. Chen.A serial 4DCT study to quantify range v*ariations in charged particle radiotherapy of 55, 309–319, 2014.

Thomas Bortfeld and Wolfgang Schlegel, *An analytical approximation of depth–dose distributions for therapeutic proton beams*. Phys. Med. Biol. 41:1331-1339, January 1996.

Yoichi Watanabe, Derivation of linear attenuation coefficients from CT numbers for low-energy photons, 1999, Phys. Med.

Thank you so much for your attention/time!

Questions?

Edge detection through two Bragg peaks: theoretical formulation

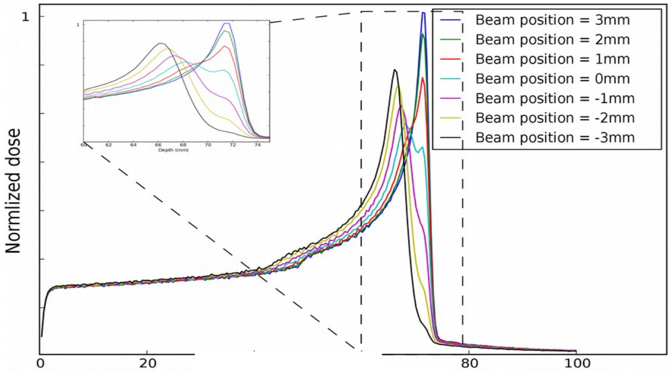

FWHM=4mm

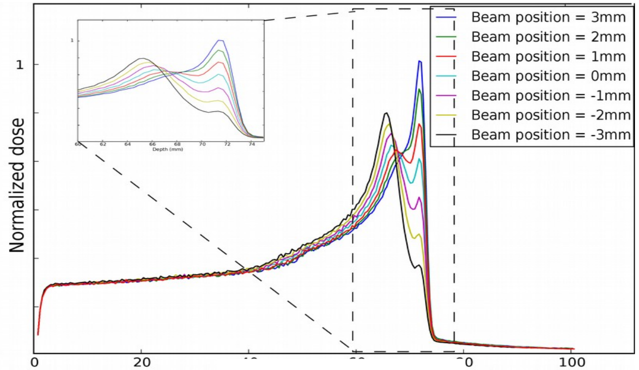

FWHM=8mm

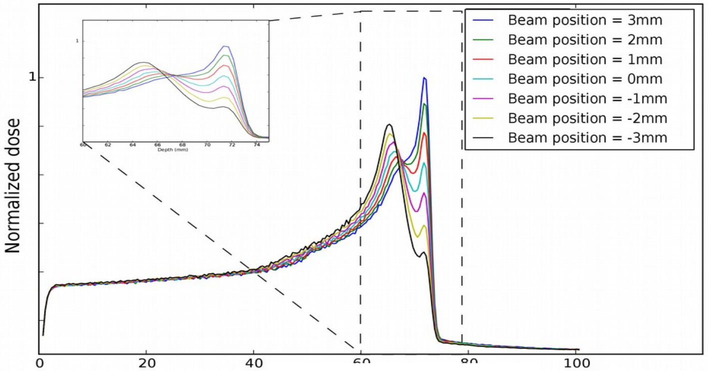

FWHM=10mm

Semi-cylindrical insert

- Smeared BP
- Different BP position
- Larger FWHM → Larger the ΔWEPL
- Larger FWHM → easier BP identification

Validation: Validation with ray-tracing

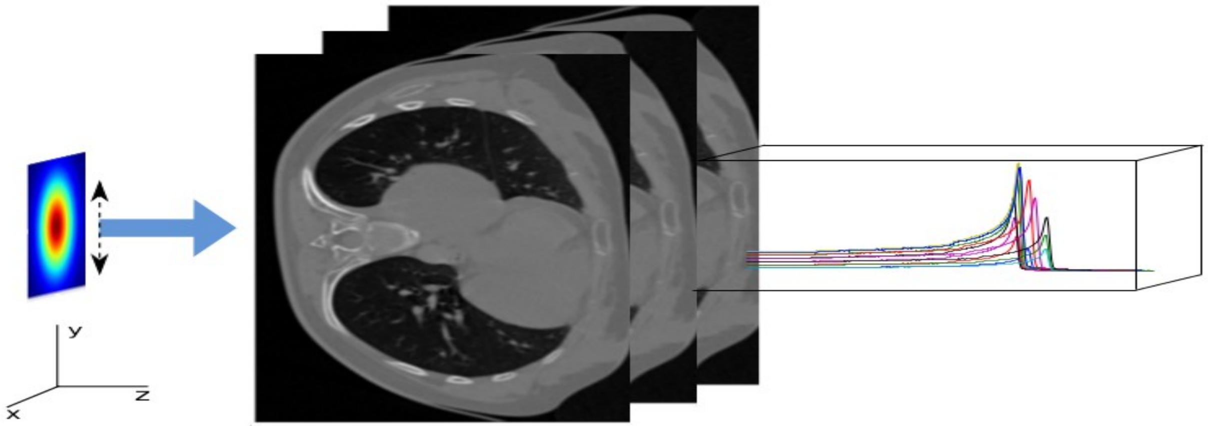

- HU-RSP calibration curve → $WET = \sum (RSP_i \times a_i)$
- Patient CT data (Cancer Imaging Archive)
- FWHM=4mm
- Beam position: [-3,-2,-1,0,1,2,3]mm above and below the interface

→ Measured signal with range dilution effects